Gold line array electrodes increase substrate affinity and current density of electricity-producing *G. sulfurreducens* biofilms

Ying Liu,[a] Hosaeng Kim,[b] Rhonda Franklin[b] and Daniel R. Bond*[ac]

Received 8th July 2010, Accepted 25th August 2010
DOI: 10.1039/c0ee00242a

During growth of *Geobacter* species able to transfer electrons to electrodes, biofilms consisting of multiple cell layers accumulate on surfaces. These biofilms require pathways for efficient electron relay towards the electrode, and diffusion of protons and end products away from the electrode. We hypothesized that altering the geometry of current-collecting electrodes would improve diffusion of substrates into electricity-producing biofilms, and allow testing of hypotheses related to the limits of long-range electron transfer. Two designs exposing equal gold surface areas to cultures of *Geobacter sulfurreducens* were compared: one consisting of a rectangular gold electrode and the other an array of 10 μm wide lines separated by 100 μm of non-conductive material. In all experiments, the line array electrode stabilized at a current density 4-fold higher (per unit electrode surface area) after 140 h of growth (1600 μA cm^{-2} *vs.* 400 μA cm^{-2}). Confocal imaging and cyclic voltammetry analysis demonstrated that because cells could grow at least 15 μm outward in a semicylinder from the gold lines, 4-fold more biomass could share each line electrode, compared to the rectangular geometry. The semicylinder-shaped biofilms did not fill in gaps between the electrodes after 300 h of growth, suggesting a limitation to the distance of useful between-cell electron transfer. The wider spacing of biofilms also improved the affinity of cells for acetate, especially under quiescent conditions.

Introduction

Some bacterial species possess mechanisms for transferring electrons from oxidative internal reactions to the outer cell surface, where they can be used to reduce metals, dyes, and petroleum hydrocarbons. This suggests many new strategies for energy generation, bioremediation, and sensing, in which bacteria self-assemble on an electrode surface to couple complex oxidation or reduction reactions to efficient electron transfer. The challenges related to harnessing bacteria, primarily for fuel-cell like devices, have been detailed in multiple reviews,[1–6] and a recent text.[7]

The transfer of electrons across multiple cell membranes (a span of over 100 Å) is a feat requiring several interacting redox proteins. Similarly, attachment of multiple bacterial layers to electrodes, to achieve the high current densities produced by strains in the genus *Geobacter* (~1 mA cm^{-2}), is the sum of additional protein–protein interactions. The organisms in the initial layer must bring redox proteins in contact with the electrode, then also serve as the "electrode" for additional layers, relaying electrons along a biological matrix. Previous work has suggested that, for *Geobacter*, growth of approximately the first 10 cell thicknesses (or 10 μm) proportionally increases current density, providing strong evidence for such cell–cell electron relay.[8] At a crucial distance, cell–cell layering no longer increases the net current production. Different theories have been proposed to explain the mechanism of the *Geobacter* cell–cell conductivity, as well as the ultimate factors limiting the distance cells can relay electrons to the electrode. These are primarily separated into conductivity issues (kinetics of the electron conduit carrying electrons to the electrode) and ionic issues (proton or charge diffusion away from the electrode).[9,10]

Many applications harnessing bacteria as electrode catalysts have increased current density per unit volume by filling reactors with porous and heterogeneous high surface area electrodes. However, to study the biochemical and biophysical mechanisms that control diffusion and electron transfer within *Geobacter* biofilms, it is desirable to create controlled environments where each cell experiences similar conditions. Such conditions should increase the current output per unit surface area. In addition, if microbial biocatalysts are to be used in sensory or detection systems, mass transfer conditions and the exposed surface area of the biofilm should be controlled.

In this report, we describe fabrication of gold electrodes consisting of equal surface areas, designed to allow growth of *Geobacter sulfurreducens* as a planar film or as a series of isolated thin lines. The catalytic and non-catalytic voltammograms from the microbial films were similar to what has been observed with planar graphite electrodes. However, biofilms assembled on gold line electrodes achieved over 4-fold higher current density, a result which could be explained by biofilm conductivity allowing extension of cells beyond the electrode rather than increased diffusion. These results provide a basis for smaller and more defined arrays of microfabricated electrodes, studies with interdigitated arrays, and more controlled growth of microbial-surface interactions.

[a]*BioTechnology Institute, University of Minnesota, 140 Gortner Laboratory, 1479 Gortner Ave, St Paul, MN, 55108, USA. E-mail: dbond@umn.edu; Fax: +1 612-625-1700; Tel: +1 612-624-8619*
[b]*Department of Electrical Engineering and Computer Science, University of Minnesota, Minneapolis, Minnesota, 55455, USA*
[c]*Department of Microbiology, University of Minnesota, Minneapolis, Minnesota, 55455, USA*

Experimental

Bacterial strain and culture media

G. sulfurreducens strain PCA (ATCC 51573) was cultured as previously reported[11,12] in our laboratory at 30 °C using a vitamin-free anaerobic medium containing the following per litre: 0.38 g KCl, 0.2 g NH_4Cl, 0.069 g $NaH_2PO_4 \cdot H_2O$, 0.04 g $CaCl_2 \cdot 2H_2O$, 0.2 g $MgSO_4 \cdot 7H_2O$, and 10 ml of a mineral mix [containing 0.1 g $MnCl_2 \cdot 4H_2O$, 0.3 g $FeSO_4 \cdot 7H_2O$, 0.17 g $CoCl_2 \cdot 6H_2O$, 0.1 g $ZnCl_2$, 0.04 g $CuSO_4 \cdot 5H_2O$, 0.005 g $AlK(SO_4)_2 \cdot 12H_2O$, 0.005 g H_3BO_3, 0.09 g Na_2MoO_4, 0.12 g $NiCl_2$, 0.02 g $NaWO_4 \cdot 2H_2O$, and 0.10 g Na_2SeO_4 per litre]. Unless otherwise indicated, acetate was provided as an electron donor at 30 mM. All media were adjusted to pH 6.8 prior to the addition of 2 g l^{-1} $NaHCO_3$ and were flushed with oxygen-free N_2–CO_2 (80 : 20 [vol/vol]) prior to sealing with butyl rubber stoppers and autoclaving. All experiments were initiated by inoculating with 40% (vol/vol) of cells within 3 h of reaching maximum optical density (OD > 0.6) in the medium described, with 40 mM fumarate as the electron acceptor.

Gold electrode preparation

Gold electrodes were made by electroplating gold onto a silicon wafer (thickness 480–520 μm, resistivity 1–10 ohm cm, crystal orientation ⟨100⟩, type: P, and dopant: boron). The wafer was first cleaned with sulfuric acid to remove contaminants. A silicon oxide layer was grown on top of the wafer to a thickness of ~0.5 μm by heating at 1150 °C for 90 minutes in a Tylan Atmospheric Furnace. A titanium layer of 40 nm was sputtered on top of the silicon oxide layer using an AJA International ATC 2000 Sputtering System (AJA International, North Scituate, Massachusetts). Next, a layer of gold was sputtered on top of the titanium to a thickness of 150 nm. A layer of gold was then electroplated to a thickness of 700–750 μm using a current density of 1 mA cm^{-2} in pH 6.0 K $Au(CN)_2$ solution to plate the wafers (~15 minutes). Two different patterns of gold were deposited: one was an array of 96 gold lines, each 10 μm wide and 1.5 cm long with an average height of 0.75 μm, spaced 100 μm apart (referred to as the line array). The other was a 1.5 cm long rectangular gold electrode, 0.12 cm wide. Images of each electrode are shown in Fig. 1.

The geometric surface area for the line array (accounting for the entire exposed top and three raised side edges) and the rectangular electrode was 0.173 and 0.18 cm^2 respectively. Prior to each use, electrodes were cleaned with acetone and HCl, and then cleaned electrochemically by cycling between 0.24 and 1.74 V (*vs.* SHE) in 0.5 M H_2SO_4 until a characteristic cyclic voltammogram of a gold surface was obtained. Poor cleaning, due to residual biomass or other contaminants on the surface, was evident during this electrochemical cycling, and preliminary results showed that this cleaning step was essential for repeatable results and uniform growth.

Bioreactor assembly

The three-electrode system was used in all electrochemical experiments. Two working electrodes, one of each geometry, were incubated in each reactor, and controlled by a different potentiostat channel. A graphite plate and a calomel reference electrode (Fisher Scientific, Pittsburg, PA) consisting of mercury/mercurous chloride and saturated potassium chloride, SCE (0.244 V *vs.* standard hydrogen electrode, SHE), were used as a common counter electrode and a reference electrode, respectively. The 20 ml conical vessel with a custom-made Teflon lid (BioAnalytical Systems, West Lafayette, IN), a magnetic stir bar, and reference electrodes in connection with a salt bridge assembled from a 3 mm Vycor frit (BioAnalytical Systems, West Lafayette, IN) and a 3 mm glass capillary filled with 0.1 M Na_2SO_4 in 1% agar were constructed as previously described.[8,11,12] All of the reactors were placed in a water bath to maintain cells at 30 °C under a constant flow of sterile humidified N_2–CO_2 (80 : 20 [vol/vol]) which had been passed over a heated copper column to remove trace oxygen. Chronoamperometry (CA) was performed on a 16-channel potentiostat (VMP, Bio-Logic, Knoxville, TN) and cyclic voltammetry (CV) was conducted using a Gamry PCI4 Femtostat (Gamry Instruments, Warminster, PA).

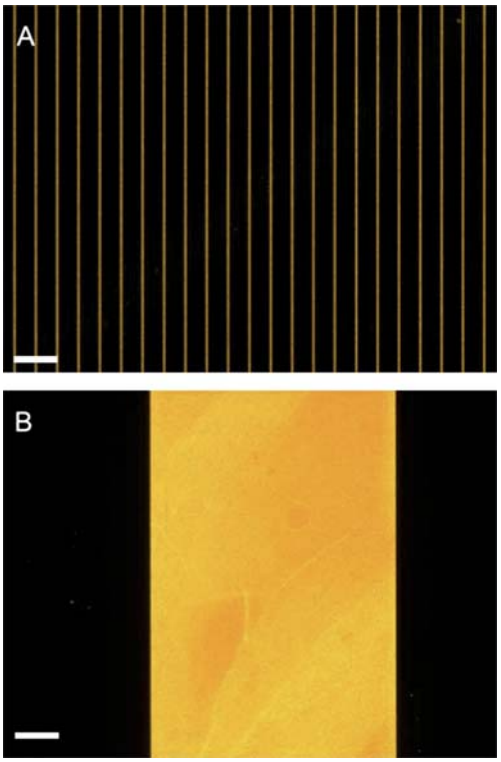

Fig. 1 Photomicrographs of 0.173 cm^2 line array electrode (A) and 0.18 cm^2 rectangular electrode (B), scale bar is 200 μm.

Biofilm growth

A 40% inoculum of stationary-phase (electron acceptor-limited) *G. sulfurreducens* was allowed to colonize gold electrodes poised at +0.24 V (*vs.* SHE) using chronoamperometry. To halt biofilm growth at different growth phases, medium was replaced with donor-free medium, and incubated poised at +0.24 V (*vs.* SHE) until substrates were depleted (typically 24 h, or until background current stabilized below 0.5 μA). All operations were

done in strictly anaerobic conditions, in reactors containing one electrode of each geometry.

Scanning electron microscopy (SEM) and confocal laser scanning microscopy analysis

The biofilms were examined using a S3500N SEM (Hitachi, Japan). Samples were fixed in 2.5% glutaraldehyde in 0.1 M phosphate, pH 7.4, washed three times in buffer supplemented with 1% OsO_4, dehydrated stepwise in a graded series of aqueous ethanol solutions (25, 50, 75, 85, 95, and 100%) for 10 min, and then critical-point-dried. Finally, samples were sputter coated with Au prior to SEM observation in vacuum compartment and examined at an accelerating voltage of 5 kV.

A Nikon C1 spectral imaging confocal microscope (Nikon, Japan) was used to image biofilm-covered electrodes. Immediately following harvesting, the biofilm-covered electrodes were gently washed in growth medium to remove planktonic cells and then stained with the LIVE/DEAD BacLight bacterial viability kit (Invitrogen Corp., Carlsbad, CA), incubated for 30 min in the dark, rinsed with growth medium, and placed on a microscope slide. Mounting oil was used during viewing of bacteria, and two laser wavelengths, 488 and 561 nm, were used to excite the stains.

Results and discussion

Biofilm growth and general electrochemistry

The fabrication procedures were specifically designed to result in two electrodes with similar geometric surface areas for microbial colonization (Fig. 1). This was achieved either by depositing a single flat rectangular surface or by depositing a series of lines 10 μm wide which were 0.75 μm high and 100 μm apart. Taking into account the area and height of the edges, the surface area available for microbial contact and electron transfer for each electrode was similar within 0.007 cm^2.

Each experiment was conducted in a reactor that contained two electrodes (one of each design), which allowed the same culture of *G. sulfurreducens* to colonize each electrode simultaneously under identical conditions. Electrodes were maintained at a constant potential of +0.24 V *vs.* SHE,[12] during the attachment and growth phase. Within 24 h of exposure to bacteria, the exponential rate of current increase of the two electrodes was similar. As has been observed in our experiments with polished graphite electrodes, this early exponential phase continued as the biofilm progressed from densities representing a monolayer stage (less than 100 μA cm^{-2}, based on a average size for *Geobacter* of 1 μm^2, a protein : cell ratio of $\sim 0.3 \times 10^{-6}$ μg, and a conservative current : protein ratio of 5 μA:μg[8]) to a phase where cells must layer on top of each other for subsequent growth. Later in this 'stacking' phase of growth, the subsequent rise in current for both electrodes transitioned to a more linear increase, slowing until reaching a maximum at 100 h (Fig. 2A).

However, even though the two electrodes had similar geometric surface areas, the electrode consisting of an array of 10 μm wide lines supported a 4-fold higher current density (per unit gold surface area) than the rectangular electrode. This effect was observed in all experiments ($n = 4$), and was not a function of time, as both electrode configurations reached a maximum current density after 3 days of growth.

To further assess if the overall electrochemical behavior of gold-attached biofilms was similar to what has been observed for *Geobacter* colonizing other electrode materials, 1 mV s^{-1} cyclic voltammetry was performed. Fig. 2B shows representative current–voltage responses after 100 h of growth. Colonization of the line array electrodes did not alter the midpoint potential or steepness of the catalytic wave (as inferred by derivative plots of the current–voltage data), and data from all gold electrode configurations were similar to the response reported for *G. sulfurreducens* grown on graphite and other carbon electrodes.[12,13] In the presence of excess electron donor, shifting from agitation with a magnetic stir bar to quiescent conditions only lowered limiting current by 10–15% for all fully grown biofilms. Thus, while the electrode design significantly increased the overall current density, it did not alter the basic current–voltage response characteristics of biofilms or their ability to respire in the presence of excess electron donor.

Confocal laser scanning microscopy and scanning electron microscopy of biofilms

Three-dimensional imaging of biofilms provided an explanation for the higher current densities observed on the line array electrodes. Significant biofilm accumulation was only observed on sections of electrodes where gold was present to act as an electron acceptor for *Geobacter*, even after many days of growth. Above the rectangular electrode (Fig. 3A), biofilms were present as a uniform layer averaging 15 μm in thickness at 140 h. In contrast, biofilms were observed growing as semicylinders above, and around each gold line, with cells also extending 15 μm in all directions beyond the gold surface (representative images in Fig. 3B and C). An SEM image of a section, where cells were scraped away to show the relative size of the electrode and surrounding cell film, is shown in Fig. 3D.

Imaging of multiple sections of each electrode showed that the widely spaced line configuration allowed more *Geobacter* cells to utilize each unit of gold surface area, as cells could grow laterally outward as well as vertically above each electrode, in a semicylinder. Based on average measurements of biofilm thickness and geometry, the total volume of biofilm in contact with each electrode was estimated. For example, after 140 h of growth, biofilms on rectangular electrodes could be represented as a box equivalent to 2.7×10^{-4} cm^3 of biomass. Since the outer edge of the semicylindrical biofilms extended in all directions from each gold line, this allowed a 10 μm stripe of gold to act as a nearly 40 μm electrode, and allowed the total estimated volume of the biofilm to be on the order of 10.8×10^{-4} cm^3.

The ratio between these volume estimates was consistent with the ratio in current density. These measurements indicated that the arrays supported increased current density primarily by allowing more biomass per unit area, rather than by increasing the current output per unit biomass. These observations also supported two conclusions: that a mechanism exists allowing multiple layers of cells to efficiently self-exchange or relay electrons to the electrode, and that beyond approximately 15 μm, a barrier (either electron relay towards the electrode or H^+/ionic migration outward) begins to limit this mechanism of *Geobacter*

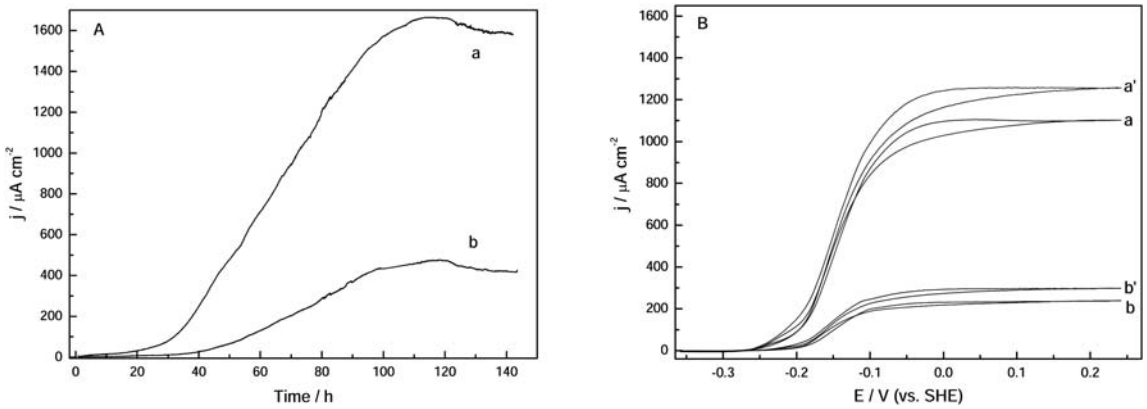

Fig. 2 Growth of representative biofilms under an applied potential of +0.242 V *vs.* SHE on gold line array electrode (curve a) and rectangular electrode (curve b) (A). Biofilm catalytic performance after 100 hours of growth in the presence of 20 mM acetate is shown in cyclic voltammograms (1 mV s^{-1}) (B) for gold line array (curves a and a′) and normal rectangular electrode (curves b and b′). Curves a and b are recorded in quiescent solution; and curves a′ and b′ are from solutions stirred with a magnetic stir bar.

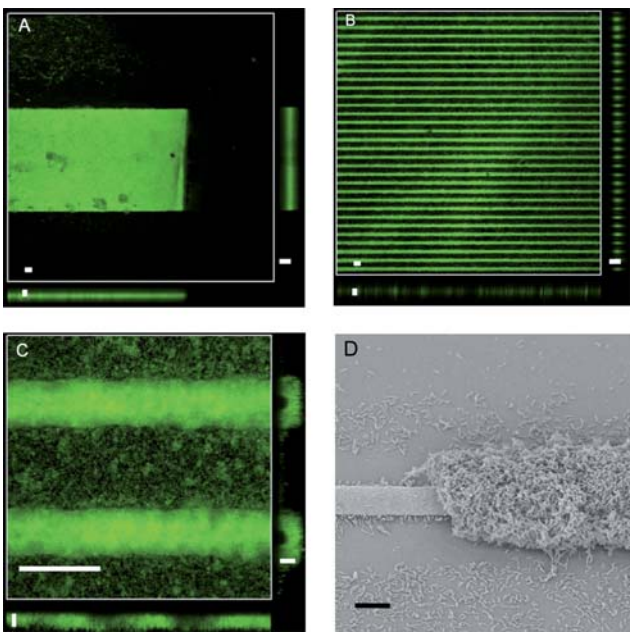

Fig. 3 Confocal laser scanning microscopy images of rectangular electrode (A) and line array electrode (B), after 140 h of colonization (4× magnification). Line array electrode is also shown at 60× magnification (C). In all confocal images, the center images are maximum top projections of all slices in the 3-dimensional stack, the smaller images (bottom and right) are orthogonal cross-sections of the biofilm. An SEM image of a single line from the array electrode (1000×) is also shown, where a section was mechanically dislodged (D). Scale bars for top views in A and B are 100 μm, and side views are 50 μm. Top view scale bar in C is 100 μm, and side scale bars are 10 μm. Scale bar in D is 10 μm.

growth. Further evaluation of these possibilities is included in the Discussion.

Single-turnover voltammetry comparisons of biofilms

While cyclic voltammetry and the ratio of biofilm mass to current density suggested that biofilms were similar, a series of experiments were conducted in the absence of electron donor to investigate possible differences in apparent charge diffusion within the biofilm. In the absence of substrates, cyclic voltammetry can reveal both the potentials and kinetics of reversible redox-active proteins on cell surfaces.[8,13] In *Geobacter*, as scan rates are increased, peak heights of the reversible reactions shift in a manner characteristic of diffusional limitations (peak height proportional to the square root of the scan rate) as opposed to complete discharge behavior characteristic of thin-film conditions which is observed with *Shewanella*.[14] As the biofilm on the electrode represents a surface-confined electrochemical process, it is expected that the peak current value should linearly increase with the elevated potential scan rate. The fact that the *Geobacter*-coated electrode does not behave in this manner is hypothesized to originate from the multiple layers of *c*-type cytochromes within the thick biofilm. Similar behavior is common in redox hydrogels with layers of mobile redox centers,[20,21] and has been observed in other *Geobacter* biofilms.[13]

All *G. sulfurreducens* biofilms grown on all gold electrode configurations, when starved free of substrates to allow investigation of reversible reactions, demonstrated this semi-infinite diffusion behavior which we have observed using graphite electrodes. The overall slope of the response was clearly steeper for the line array electrode configuration, suggesting a possible faster apparent diffusion coefficient for charge in line array biofilms (Fig. 4). However, the fact that the cells could extend 15 μm from either side of the 10 μm gold line electrodes increased the effective surface area of the line array electrode. When peak heights from both electrode configurations were normalized for this increased area term, using either integration of the peak area obtained during a 1 mV s^{-1} linear sweep voltammogram (as an estimate of the total redox-active protein in communication with the electrode) or the volume estimates (calculated from confocal analysis), the overall slope of the peak height response was similar (Fig. 4, inset uses the voltammetry normalization). Based on the standard Randles–Sevick equation defining diffusion-controlled systems,[15] this similar slope was consistent with a similar apparent diffusion coefficient for charge transfer within the matrix of both biofilms. This further supported the idea that the biofilms had grown and interconnected in a similar fashion, with the

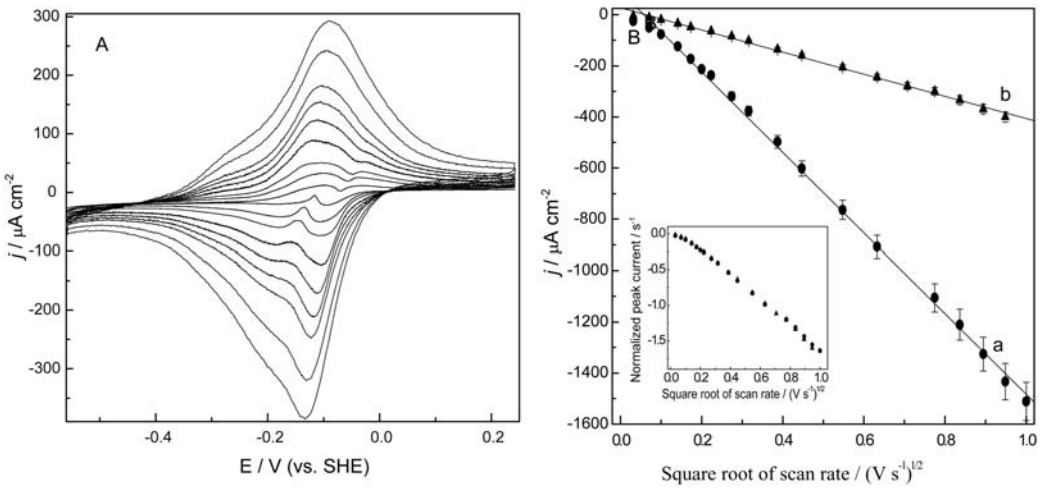

Fig. 4 Representative single-turnover cyclic voltammograms (biofilms depleted of electron donors) for gold line array electrode (A) at different scan rates (1, 5, 10, 20, 30, 40, 50, 75, and 100 mV s^{-1}); (B) linear relationship of primary cathodic peak currents with square root of scan rate on gold array electrode (a) and gold band electrode (b). Inset shows a plot of normalized cathodic peak currents, achieved by dividing peak heights by total biofilm coverage (estimated at 1 mV s^{-1}), producing a similar relationship for both gold line array (circle markers) and rectangular electrodes (triangle markers).

primary difference being simply the amount of biomass able to access each electrode.

Affinity of biofilms for acetate as a function of electrode geometry

The final hypothesis tested with these electrodes was if the change in geometry would alter diffusion of substrates into the biofilms. To obtain biofilms of differing thickness (representing average thicknesses of ~5 μm *vs.* ~15 μm based on imaging), cultures were grown for either 70 h or 140 h, depleted of intracellular and extracellular electron donors (acetate) for 12 h, and subjected to a series of increasing acetate concentrations. As before, pairs of electrodes were grown and incubated in the same reactor, to ensure each biofilm was exposed to identical bulk phase acetate concentrations and mixing conditions. After each dose of acetate, 2 mV s^{-1} cyclic voltammetry was performed to measure catalytic electron transfer and limiting current across a range of potentials. Data were also collected under stirring *vs.* quiescent conditions for each concentration.

An example series of voltammograms collected at different acetate concentrations is shown in Fig. 5. Derivative analysis of all voltammograms indicated that the midpoint potential of catalytic waves for all treatments was similar within 10 mV. Thus, the key difference between each treatment was the limiting current (measured at +0.2 V *vs.* SHE), as a function of acetate concentration.

Regardless of the stage of growth, or agitation of the medium, biofilms growing as semicylinders demonstrated a higher apparent affinity for acetate than standard rectangular configurations at all stages. Most dramatically, mature (140 h) biofilms achieved 50% maximal current density at an acetate concentration of 150 μM, while the rectangular biofilms required over 3-fold higher concentrations (500 μM) to achieve the same effect. Because the apparent affinity constant for *G. sulfurreducens* (half-maximal rate of acetate consumption) under well-mixed conditions is on the order of ~10 μM,[16] all of these values reflected effects of substrate depletion within the biofilm. However, the higher apparent affinity of the line array biofilms confirmed improved mass transport to the biofilm surface when the biofilms were spaced 100 μm apart and arranged to allow radial diffusion.

Not surprisingly, differences in affinity were less significant at early stages of growth, when biofilms were thinner and less susceptible to diffusional limitations. With stirring enabled, thin biofilms on both electrode configurations reached half-maximal current production near 150 μM, and gradually saturated at maximal rates of current production at nearly 3000 μM. Thin biofilms on line array electrodes retained this high affinity under quiescent conditions, indicating that the wide spacing of biofilms

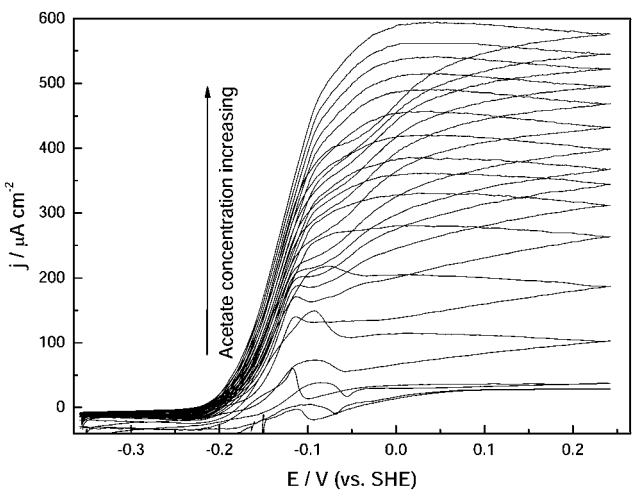

Fig. 5 Representative cyclic voltammograms (second sweep) illustrating method of determining limiting current. Data are shown from a gold line array electrode biofilm grown for 70 h, recorded at different acetate concentrations, with stirring (concentrations of 0, 20, 70, 120, 170, 220, 270, 340, 440, 640, 840 1040, 1540, 2540 and 3540 μM, respectively), scan rate is 2 mV s^{-1}. For each experiment, the limiting current was recorded and plotted as a function of acetate concentration (see Fig. 6).

reduced the formation of boundary layers that typically depleted substrates near the surface of flat electrodes.

Comparisons with planar graphite electrode biofilms

Reactions at surfaces are strongly affected by available surface area, and diffusion of substrates. In the special case of electricity-producing microbial biofilms, the relative rates that the biofilm can obtain electron donors, relay electrons to the electrode, and expel end products all can serve as bottlenecks preventing current production.[9,10,17] The experiments described here show that biofilm morphology, apparent current density, and substrate affinity of *G. sulfurreducens* can be altered by simple manipulation of its local environment. These studies also show that gold can be utilized as a robust surface for attachment, electron transfer, and growth by *G. sulfurreducens*.[18,19]

Previous work utilizing graphite and glassy carbon surfaces has suggested a model in which the final interfacial electron transfer event from *Geobacter* to electrodes is non-limiting, compared to the relative rate that electrons can be obtained from intracellular oxidation and transfer to the outer surface.[13] The fact that gold (which could alter interfacial electron transfer kinetics) did not alter the general characteristics of catalytic or non-catalytic voltammetry was consistent with this model.

A unique aspect of *Geobacter* physiology, the fact that electrons can be efficiently relayed between cells to the electrode, was also confirmed in these experiments. Regardless of the electrode geometry, cells were able to extend 15–20 μm in all directions from an accepting electrode after 140 h of growth. The ability of *G. sulfurreducens* to add 10 to 20 cell layers on top of electrodes, and proportionally increase current density, is similar to enzyme-based strategies that entrap enzymes in polymers with mediators on electrodes.[20,21] In the case of the line array electrodes, this natural conductivity was simply exploited to add enzyme in multiple dimensions.

The limits of the 'conductive' biofilm

An unanswered question related to electron transfer by *Geobacter* is an explanation for the self-limiting biofilm thickness observed on all electrodes: why does growth abruptly slow as biofilms approach 20 μm? One hypothesis driving the fabrication of these array electrodes was that, by providing additional space between biofilms, diffusion could assume a radial

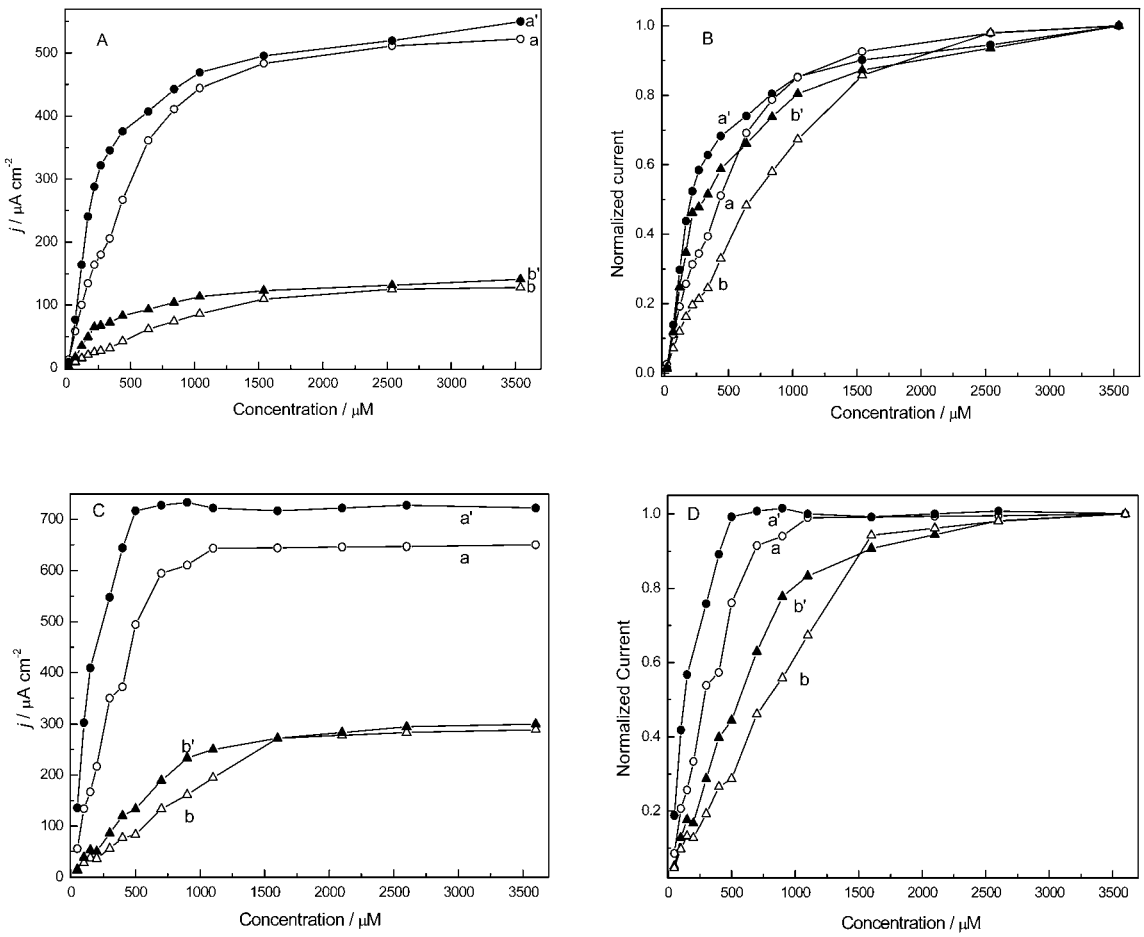

Fig. 6 Increased apparent affinity for acetate by biofilms grown on line array electrodes. Gold line array (curves a and a′) and normal rectangular electrode (curves b and b′) are shown in all figures. (A) and (B) are from biofilms grown for 70 h, while (C) and (D) are from 140 h biofilms. Curves a and b were in quiescent solution and curves a′ and b′ were under stirring conditions. (A) and (C) show raw data, as absolute catalytic current, while (B) and (D) are normalized to maximum catalytic current at saturating acetate concentrations.

or band-microelectrode pattern, to accelerate entry and exit of reactants. Evidence for this improvement in delivery from the exterior, expected from standard microelectrode diffusion equations,[15] was obvious in experiments with acetate limitation (Fig. 6). However, growth on both geometries still ceased at similar points, suggesting the limitation was inherent to the distance cells were located from an electrode, not due to diffusion of substrates within the film.

Thus, this presents an apparent contradiction. Most simply, as *G. sulfurreducens* grows on a flat surface, each new layer adds a proportional amount of additional current, demonstrating there is a mechanism of long-range conductivity transporting electrons through biofilms.[8,12,22,23] Therefore, when *G. sulfurreducens* is presented with a 1.5 × 1 cm surface, an even film of at least 15 μm is expected to form over that surface, if biofilm conductivity is not limiting. However, when the electrodes were separated by 100 μm, a biofilm did not fill in the gaps between current collecting sites, and establish this predicted layer over the array before growth was arrested. These data support a model where biofilm conductivity slows growth as cells find themselves at a crucial distance from the electrode. These data show that any model of *Geobacter* conductivity should address these limits for cooperative long-distance electron transfer.

Conclusions

Properly cleaned gold surfaces fabricated to impose unique growth patterns can be useful tools for the study of *G. sulfurreducens.* Our general observation that wider spacing of biofilms improved the overall sensitivity towards electron donors, and allowed cells to better utilize each unit of surface area, while not altering the electrochemical behavior commonly described for *Geobacter*, justifies further investigations of *Geobacter* physiology using gold surfaces. Future work should examine permutations of spacing and geometry, to more directly test the hypothesis put forward in this work that there are limits to *G. sulfurreducens* long-range electron transfer beyond distances of 20 μm unrelated to issues of acidification.[24] In addition, a shift to use of laminar flow biofilm reactors would better control the diffusion regime and allow separation of fundamental diffusional *vs.* electron transfer variables that control respiration within biofilms.

Acknowledgements

This work was supported by the National Science Foundation (ECS 0702200) and the Office of Naval Research (NM000140810162).

References

1 D. R. Lovley, *Geobiology*, 2008, **6**, 225–231.
2 D. R. Lovley, *Curr. Opin. Biotechnol.*, 2008, **19**, 564–571.
3 K. Rabaey, J. Rodriguez, L. L. Blackall, J. Keller, P. Gross, D. Batstone, W. Verstraete and K. H. Nealson, *ISME J.*, 2007, **1**, 9–18.
4 B. E. Logan and J. M. Regan, *Environ. Sci. Technol.*, 2006, **40**, 5172–5180.
5 Z. Du, H. Li and T. Gu, *Biotechnol. Adv.*, 2007, **25**, 464–482.
6 U. Schröder, *Phys. Chem. Chem. Phys.*, 2007, **9**, 2619–2629.
7 B. Logan, *Microbial Fuel Cells*, John Wiley and Sons, Hoboken, NJ, 2008.
8 E. Marsili, J. Sun and D. R. Bond, *Electroanalysis*, 2010, **22**, 865–874.
9 C. I. Torres, A. Kato Marcus and B. E. Rittmann, *Biotechnol. Bioeng.*, 2008, **100**, 872–881.
10 C. I. Torres, H. Lee and B. E. Rittmann, *Environ. Sci. Technol.*, 2008, **42**, 8773–8777.
11 E. Marsili, D. B. Baron, I. D. Shikhare, D. Coursolle, J. A. Gralnick and D. R. Bond, *Proc. Natl. Acad. Sci. U. S. A.*, 2008, **105**, 3968–3973.
12 E. Marsili, J. B. Rollefson, D. B. Baron, R. M. Hozalski and D. R. Bond, *Appl. Environ. Microbiol.*, 2008, **74**, 7329–7337.
13 H. Richter, K. P. Nevin, H. F. Jia, D. A. Lowy, D. R. Lovley and L. M. Tender, *Energy Environ. Sci.*, 2009, **2**, 506–516.
14 D. B. Baron, E. Labelle, D. Coursolle, J. A. Gralnick and D. R. Bond, *J. Biol. Chem.*, 2009, **284**, 28865–28873.
15 A. J. Bard and L. R. Faulkner, *Electrochemical Methods*, John Wiley and Sons, 2nd edn, 2001.
16 A. Esteve-Nunez, M. Rothermich, M. Sharma and D. Lovley, *Environ. Microbiol.*, 2005, **7**, 641–648.
17 C. I. Torres, A. K. Marcus, P. Parameswaran and B. E. Rittmann, *Environ. Sci. Technol.*, 2008, **42**, 6593–6597.
18 H. Richter, K. McCarthy, K. P. Nevin, J. P. Johnson, V. M. Rotello and D. R. Lovley, *Langmuir*, 2008, **24**, 4376–4379.
19 S. R. Crittenden, C. J. Sund and J. J. Sumner, *Langmuir*, 2006, **22**, 9473–9476.
20 A. Heller, *Curr. Opin. Chem. Biol.*, 2006, **10**, 664–672.
21 F. Mao, N. Mano and A. Heller, *J. Am. Chem. Soc.*, 2003, **125**, 4951–4957.
22 G. Reguera, K. P. Nevin, J. S. Nicoll, S. F. Covalla, T. L. Woodard and D. R. Lovley, *Appl. Environ. Microbiol.*, 2006, **72**, 7345–7348.
23 A. Kato Marcus, C. I. Torres and B. E. Rittmann, *Biotechnol. Bioeng.*, 2007, **98**, 1171–1182.
24 A. E. Franks, K. P. Nevin, H. F. Jia, M. Izallalen, T. L. Woodard and D. R. Lovley, *Energy Environ. Sci.*, 2009, **2**, 113–119.

